



Research paper

Flexible, thermal processable, self-healing, and fully bio-based starch plastics by constructing dynamic imine network

Xiaoqian Zhang, Haishan Zhang, Guowen Zhou, Zhiping Su, Xiaohui Wang*

State Key Laboratory of Pulp and Paper Engineering, South China University of Technology, Guangzhou 510640, China

Received 3 April 2023; revised 19 June 2023; accepted 18 August 2023

Available online ■ ■ ■

Abstract

The serious environmental threat caused by petroleum-based plastics has spurred more researches in developing substitutes from renewable sources. Starch is desirable for fabricating bioplastic due to its abundance and renewable nature. However, limitations such as brittleness, hydrophilicity, and thermal properties restrict its widespread application. To overcome these issues, covalent adaptable network was constructed to fabricate a fully bio-based starch plastic with multiple advantages via Schiff base reactions. This strategy endowed starch plastic with excellent thermal processability, as evidenced by a low glass transition temperature ($T_g = 20.15\text{ }^\circ\text{C}$). Through introducing Priamine with long carbon chains, the starch plastic demonstrated superior flexibility (elongation at break = 45.2%) and waterproof capability (water contact angle = 109.2°). Besides, it possessed a good thermal stability and self-adaptability, as well as solvent resistance and chemical degradability. This work provides a promising method to fabricate fully bio-based plastics as alternative to petroleum-based plastics.

© 2023 Institute of Process Engineering, Chinese Academy of Sciences. Publishing services by Elsevier B.V. on behalf of KeAi Communications Co., Ltd. This is an open access article under the CC BY-NC-ND license (<http://creativecommons.org/licenses/by-nc-nd/4.0/>).

Keywords: Bioplastic; Covalent adaptable networks; Schiff base chemistry; Thermal processability; Self-healing

1. Introduction

Petroleum-based plastics have been widely used not only in industry but also in our daily life [1,2]. Despite the numerous benefits plastics have provided, their production, application, and disposal are not sustainable. Due to the persistence and low recycling rate, plastics have been transferring from land into ocean and have accumulated within our food chain, posing a serious threat to environment and human health [3,4]. Therefore, development of renewable, low-cost, and eco-friendly alternative materials has drawn increasing attention and interests.

Starch-based plastics exhibit great potential to replace petroleum-based plastics. Since it is the second most abundant biopolymer on earth, approximately 50% of the commercial

bioplastics are fabricated from starch [5]. The cost-efficient and scalable conventional starch-based plastics have been utilized in a variety of fields [6–8]. However, they still face some major challenges, such as high hydrophilicity, poor thermal processability, and unsatisfactory mechanical behaviors [9]. Various strategies have been investigated to overcome these limitations, including physical/chemical modifications of starch [10–12], reinforcement with other polymers or nanoparticles [13–16], and addition of plasticizers [17,18]. Although some of the approaches have resulted in improved properties, a great deal of efforts is still required to develop high-performance starch-based plastics.

Recently, covalent adaptable networks (CANs) have been constructed in polymers combining the advantages of traditional thermosets and thermoplastics [19–21]. The dynamics of reversible covalent bonds and mobility of polymer chains in CANs endow materials with superior mechanical quality, reprocessability, and malleability [22,23]. Various reversible covalent interactions have been used to design CANs

* Corresponding author.

E-mail address: fewangxh@scut.edu.cn (X. Wang).

polymers, such as Diels–Alder reaction [24,25], boroxine chemistry [26], disulfide chemistry [27], and transesterification [28,29]. Among them, imine bond has emerged as a remarkably diverse and useful one. The reversible nature of imine bond provides polyimines with many well-demonstrated functionalities, including malleable, processable, and recyclable [30–32]. Our team previously developed a starch-based plastic with comparable mechanical strength to some commercial petroleum-based plastics by constructing dynamic imine networks [33]. This suggests the potential of starch for fabricating bioplastics with excellent mechanical properties and a series of self-adaptability characteristics. However, the diamine monomers used in the hybridization were derived from petrochemical resources, which contradicted the idea of environmental safety. Meanwhile, this starch-based plastic still had limitations, such as a high T_g (107–190 °C) and poor flexibility (elongation at break within 3.5–7.3%). Therefore, it is meaningful to continue developing sustainable starch-based bioplastics with improved performances.

Herein, we developed a starch-based dynamic covalent crosslinking polymer, which could be used as a new bioplastic. Dialdehyde starch (DAS) was reacted with a plant oil-based diamine (Priamine) via a mild Schiff base reaction to obtain a fully bio-based starch plastic (DAS-Bio-PI). It is expected that the incorporation of dynamic imine linkages could significantly weaken the strong hydrogen bonding and enhance stress relaxation of starch chains. The influence of imine bond with heat-induced dynamic exchange property on thermal processability was then explored. Moreover, we investigated the mechanical, thermal, and degradable characteristics of this starch bioplastic. The information obtained from this work may lead to the development of fully bio-based CANs polymers potential for sustainable and renewable circular materials.

2. Results and discussion

2.1. Preparation and characterization of DAS-Bio-PI

The design strategy for the synthesis of DAS-Bio-PI is illustrated in Schematic 1. Due to the strong hydrogen bonding of molecular chains, native starch shows great stiffness, leading to the difficulties in thermal processing. We firstly converted native starch into more amorphous DAS in which the motility of molecular chains was enhanced via the cleavage of C-2 and C-3 bond of the anhydroglucose units by periodate oxidation [34]. Priamine 1074, a 100% renewable diamine monomer, is derived from natural fatty acids of vegetable oils, such as soybean oil and sunflower oil. A fully bio-based DAS polyimine was then prepared by dynamic imine chemistry from these two sustainable raw ingredients, DAS and Priamine 1074. The Schiff base reaction offered a one-step synthesis under mild conditions without any external catalyst. Dynamic imine bonds could be reversibly cleaved and reformed under heat stimulation [35], giving rise to the excellent thermal processability of DAS-Bio-PI. Therefore, DAS-Bio-PI powders could be easily thermo-processed into

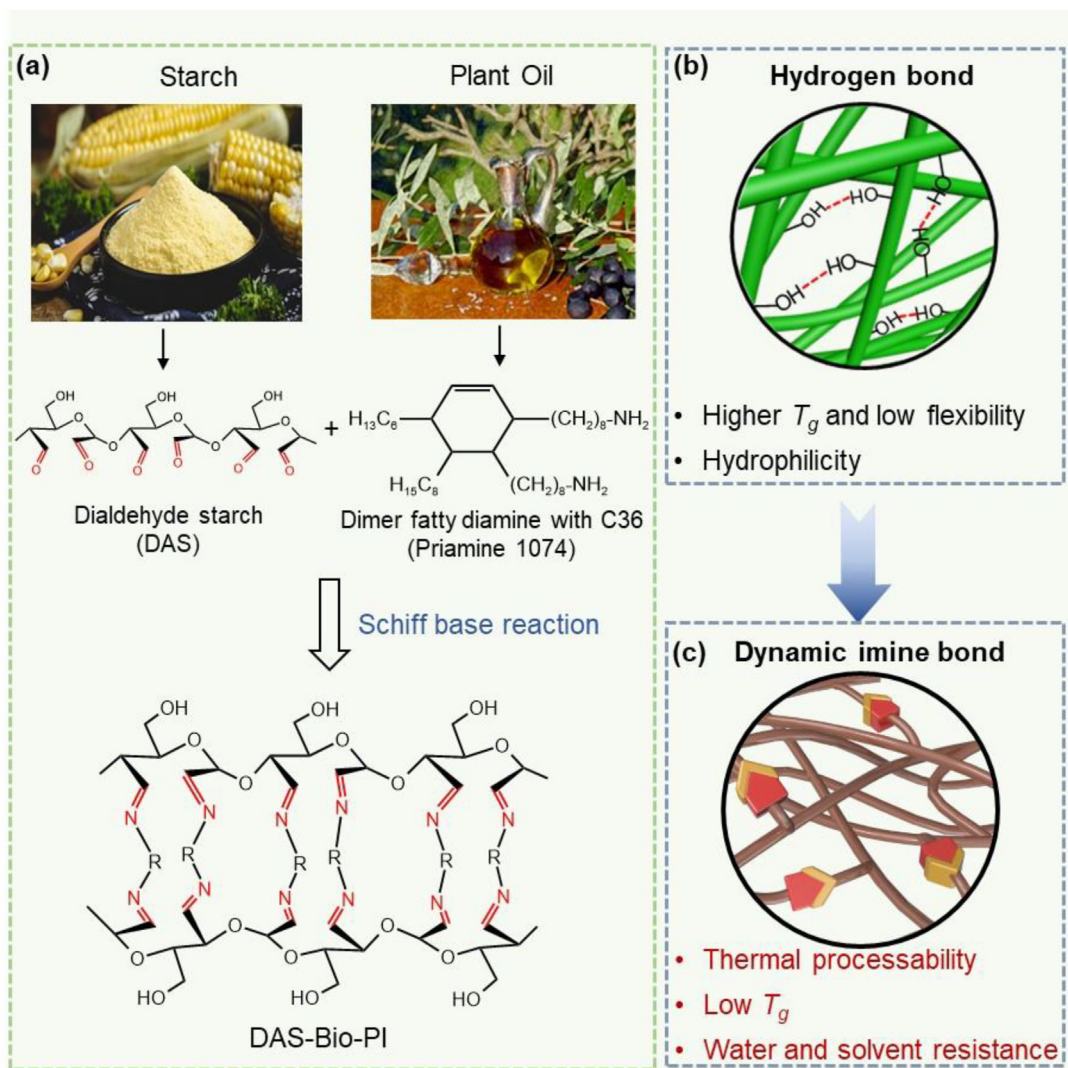
film in the absence of plasticizers by a simple heat-pressing process (30 MPa under 70 °C for 15 min). Furthermore, the steric hinderance of DAS molecule chains were boosted by the long aliphatic chains of Priamine, which enhanced the flexibility and hydrophobicity of DAS-Bio-PI.

The successful incorporation of Priamine into DAS through Schiff base reaction was confirmed by fourier-transform infrared (FT-IR) spectrums and X-ray photoelectron spectroscopy (XPS) results. In the FT-IR spectra of DAS (Fig. 1a), characteristic peak at 1734 cm^{-1} was ascribed to the aldehyde groups (-CHO). After crosslinking, the peak at 1734 cm^{-1} disappeared and characteristic peak at 1650 cm^{-1} corresponding to imine groups (-C=N-) was observed in spectra of DAS-Bio-PI. This implied that aldehyde groups were completely consumed and imine linkages were formed after polymerization [22]. In addition, DAS-Bio-PI exhibited a strong absorption peak at 2850 cm^{-1} , which belonged to stretching vibration of -CH₂- in Priamine [36]. The XPS full spectra showed that C 1s, N 1s, and O 1s were detected in DAS-Bio-PI samples (Fig. S1). With the introduction of Priamine, the content of N element increased from 0.16% to 1.74% (Table S1). Besides, the high-resolution XPS spectra of N 1s revealed three peaks at 398.93 eV, 399.94 eV, and 401.91 eV, which were assigned to N-C, N-H, and N=C, respectively (Fig. 1b).

The X-ray diffraction (XRD) curves of DAS and DAS-Bio-PI are presented in Fig. S2. Because of Priamine's side aliphatic chains that destructed crystallization and disrupted the hydrogen bonds between -OH groups [37], DAS-Bio-PI was amorphous. The micromorphology of DAS-Bio-PI powder and DAS-Bio-PI film was determined by scanning electron microscope (SEM). As depicted in Fig. S3, the DAS-Bio-PI powder was consisted of irregular and rough particles. However, these powders tuned to be an even and smooth film with a dense and continuous inner structure after heat-pressing treatment (Fig. 1c and d). In addition, 3D surface profile images (Fig. S4) also confirmed the smooth surface of DAS-Bio-PI films with root-mean-square (RMS) as small as 244.9 nm. This indicated that DAS-Bio-PI demonstrated a superior malleability enabled by dynamic imine network. The energy dispersive spectrometer (EDS) results illustrated that C, N, and O elements were distributed uniformly on the surface (Fig. S5a-c) and in the cross-section of DAS-Bio-PI films (Fig. S5d-f). Meanwhile, the presence of N element provided obvious evidence for the successful cross-linking of Priamine with DAS, which was in agreement with FT-IR and XPS analysis.

2.2. Optical and mechanical performance of DAS-Bio-PI

The DAS-Bio-PI film exhibited approximately 8-fold greater transmittance at 700 nm compared with commercial PLA plastics (Fig. 2a). The transmittance of DAS-Bio-PI film was 43.1%, 84.9%, and 87.2% when the wavelength was 600 nm, 800 nm, and 1000 nm, respectively. Fig. 2b provided a visual example showing high transparency of as-prepared



Schematic 1. Structural design strategy of DAS-Bio-PI. (a) Schematic diagram of DAS-Bio-PI via Schiff base reaction; (b) rigid and non-processable hydrogen bond in native starch; (c) thermal processable dynamic imine bonds in DAS-Bio-PI.

DAS-Bio-PI film, which could be a potential candidate for petroleum-based plastic in light management.

Tensile stress-strain curves of DAS-Bio-PI films with different reaction ratios of amino and aldehyde groups were measured. When the ratio of amino to aldehyde was 1:1, the obtained DAS-Bio-PI-1 exhibited the best mechanical performances with tensile strength, Young's modulus, and elongation at break of 5.40 ± 0.3 MPa, 21.5 ± 2.5 MPa, and $45.2\% \pm 2.2\%$, respectively (Fig. 2c and d). This might be attributed to a stable dynamic imine crosslinking network formed in DAS-Bio-PI-1. Notably, tensile strength and Young's modulus declined with the rise of amino to aldehyde ratios. When integrating more Priamine, excess of free amino group led to a decreased cross-linking density and significant declined mechanical properties [38]. Moreover, DAS-Bio-PI films exhibited excellent flexibility and toughness. These films could be easily rolled without breaking and conformably folded into different shapes (Fig. 2e).

2.3. Thermal mechanical properties and thermal stability of DAS-Bio-PI

Dynamic thermal mechanical properties and glass transition temperature (T_g) were studied by dynamic thermal mechanical analyzer (DMA). With the increase of temperature, the storage modulus of DAS-Bio-PI gradually decreased (Fig. 3a). This might be because the dynamic exchange reaction of imine bonds was triggered by increased temperature, which accelerated the mobility of the polymer chain in DAS-Bio-PI [33]. Meanwhile, no substantial change of loss modulus was observed. Samples showed one single Tan delta peak, suggesting the polymer network of DAS-Bio-PI was amorphous. This was consistent with the XRD analysis. It can be seen from Tan delta curve that T_g of DAS-Bio-PI was 20.15 °C, which was similar to those reported for polypropylene. This indicated that DAS-Bio-PI exhibited excellent thermal processability.

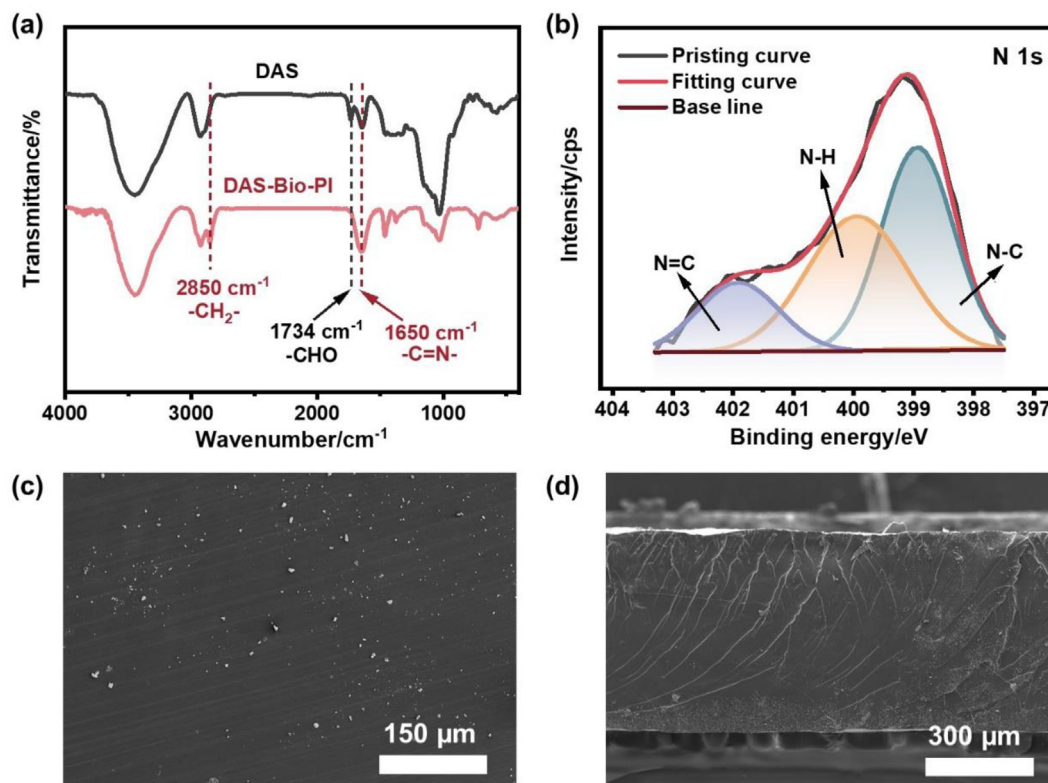


Fig. 1. Characterizations of DAS-Bio-PI. (a) FT-IR spectra and (b) N 1s high-resolution XPS spectra of DAS-Bio-PI; SEM image of (c) surface and (d) cross-section of DAS-Bio-PI films.

DAS-Bio-PI films were analyzed for time- and temperature-dependent stress relaxation at various temperatures (Fig. 3b). The relaxation time (τ), known as the time when the samples relaxed to $1/e$ of the initial modulus, was 33.4 min at 30 °C, 12.0 min at 40 °C, 9.9 min at 50 °C, 6.5 min at 60 °C, and 5.7 min at 70 °C, respectively. The increase in temperature resulted in shorter relaxation time, also suggesting the excellent thermal processability of DAS-Bio-PI. The activation energy obtained from stress relaxation for DAS-Bio-PI was determined to be 23.9 kJ mol⁻¹ (Fig. S6), which was much lower than that of previously reported polyimine networks (33.6–157.2 kJ mol⁻¹) [22,38]. With the integration of Priamine composed of long aliphatic chains, DAS-Bio-PI exhibited much faster imine exchange rate and improved mobility of molecular chains. In such case, DAS-Bio-PI could demonstrate a good flexibility without the addition of plasticizers.

DAS-Bio-PI films exhibited a superior thermal stability. Fig. 3c and d demonstrated the TGA and DTG curves of DAS and DAS-Bio-PI, respectively. It could be seen that DAS experienced one stage of thermal decomposition, starting at 250 °C and reaching maximum degradation rate at 300 °C. The thermal degradation process of DAS-Bio-PI comprised two steps, occurring at 200–400 °C and 400–500 °C, which was caused by thermal scission of starch and thermal decomposition of polymer network, respectively. The degradation temperature at 5% and 50% weight loss for DAS-Bio-PI was 240 °C and 455 °C, respectively. The maximum thermal decomposition temperature of DAS-Bio-PI was higher than that of DAS, indicating that DAS-Bio-PI had a better

thermal stability. This might be attributed to the construction of dynamic covalent cross-linked network in DAS-Bio-PI, enhancing its resistance to thermal degradation [33,39]. Besides, it was noticed that PP and PLA was completely melted at 300 °C, on the contrary DAS-Bio-PI films still had no significant dimensional changes (Fig. 3e and f). The above results demonstrated that DAS-Bio-PI in this study could be more stable under high temperature application scenarios.

2.4. Self-healing capability of DAS-Bio-PI

DAS-Bio-PI containing imine bond with dynamic exchange characteristics was expected to exhibit self-healing capability. The scratched self-healing test was firstly carried out and the process was shown in Fig. 4a. Deep cut cracks were observed on the surface of DAS-Bio-PI films scratched with a blade. By heat-pressing at 70 °C and 10 MPa for 15 min, the scratches could be invisible and re-healed. The self-healing capability was quantitatively assessed by tensile experiments. After heat-pressed for 15 min, the re-healed films exhibited a tensile strength of 5.11 MPa, an elongation at break of 39.8%, and a Young's modulus of 19.7 MPa (Fig. 4b). The recovery ratio for tensile strength, elongation at break, and Young's modulus reached 87.5%, 92.9%, and 94.5%, respectively (Fig. 4c). The increasing temperature effectively accelerated the exchange reaction of imine bonds, thereby facilitating repair process at interfaces that needed healing [39].

The self-healing ability of DAS-Bio-PI was further evaluated by large-area damage reparability test. A 10 mm × 10 mm

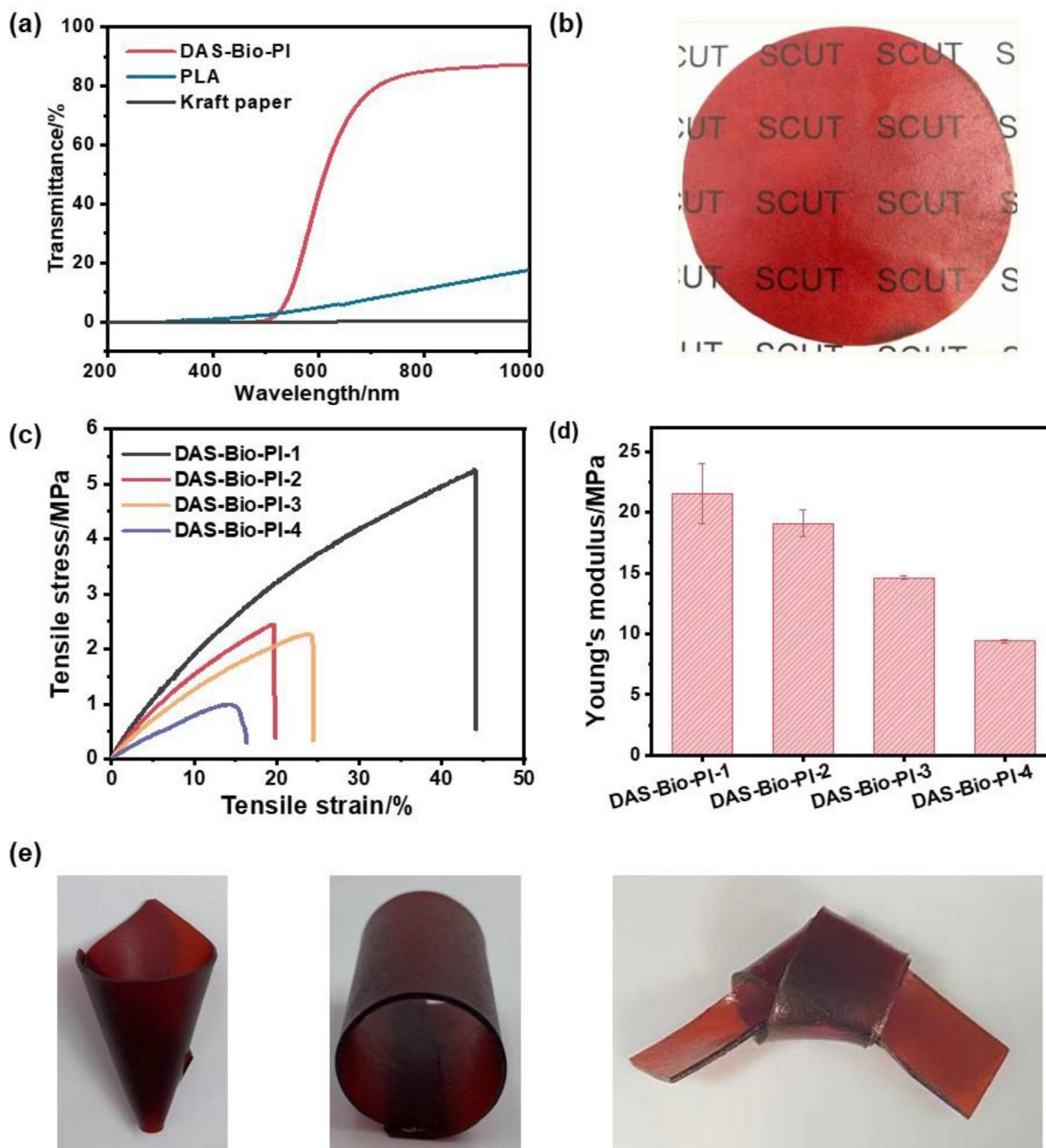


Fig. 2. Optical and mechanical properties of DAS-Bio-PI films. (a) UV transmittance curves of DAS-Bio-PI, PLA, and kraft paper; (b) photograph of DAS-Bio-PI film; (c) tensile stress–strain curves and (d) Young's modulus of DAS-Bio-PI with different ratios of amino groups to aldehyde groups; (e) photographs of folding DAS-Bio-PI films with different shapes.

large-scale damage was healed by filling up with DAS-Bio-PI powder and compression molding at 70 °C and 10 MPa. After 15 min, the re-healed area was completely integrated with the original area (Fig. 4d), suggesting damaged DAS-Bio-PI films were repaired. The self-healing efficiency reached more than 88% in terms of Young's modulus (>95%), elongation at break (93%), and tensile strength (88%) (Fig. 4e and f). These results showed a remarkable heat-induced self-healing ability of DAS-Bio-PI films.

2.5. Durability and degradability of DAS-Bio-PI

The waterproof performances and chemical resistances of DAS-Bio-PI were evaluated. DAS-Bio-PI films exhibited superior water resistance with a water contact angle of 109.2° (Fig. 5a) and an effective waterproof duration of 2 h (Fig. 5b). Moreover, the water resistance test proved that DAS-Bio-PI films could preserve their original forms quite well after soaking in water for 7 days (Fig. 5c). The excellent water

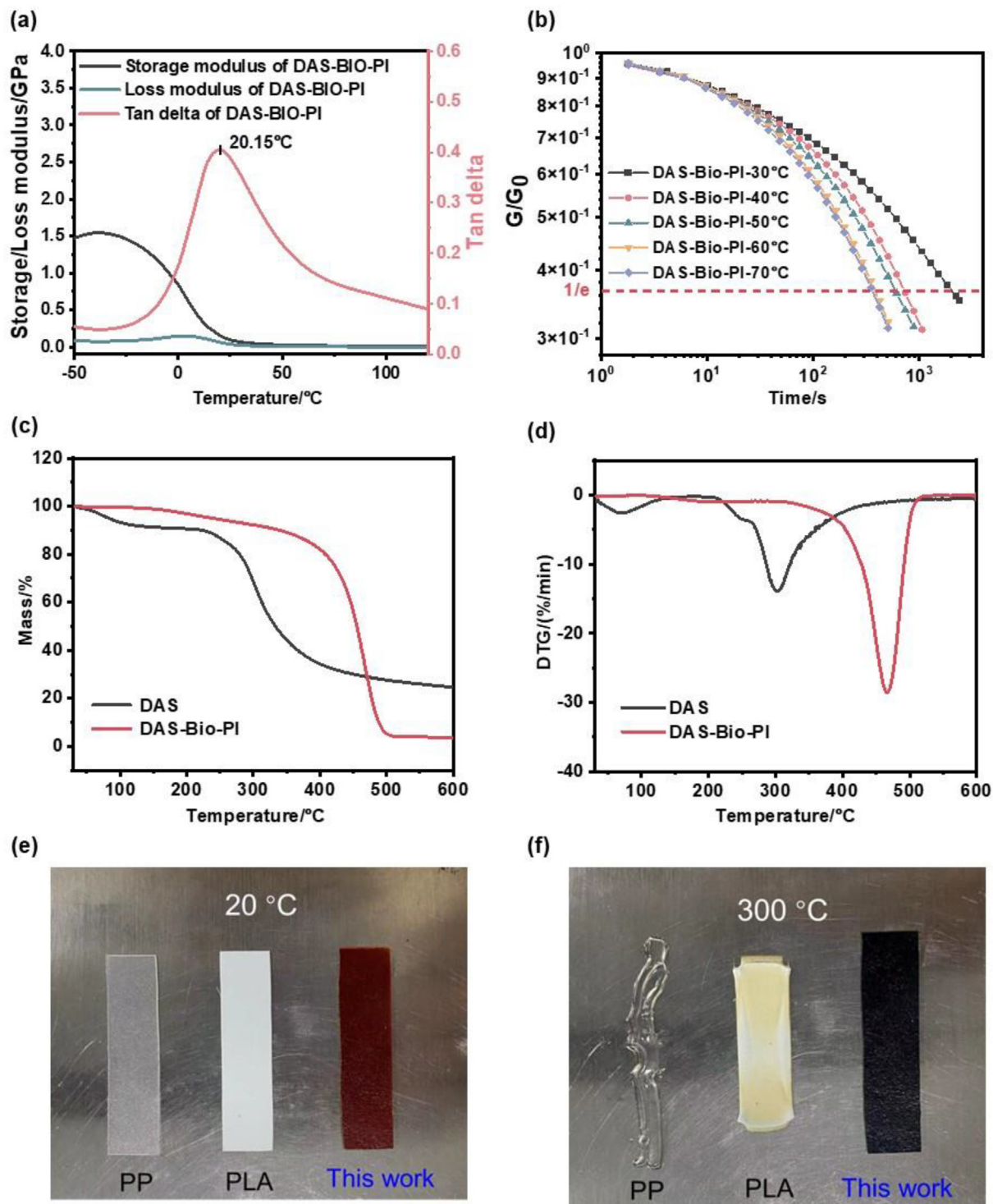


Fig. 3. Thermal mechanical properties and thermal stability of DAS-Bio-PI films. (a) Storage/loss modulus and Tan delta curves of DAS-Bio-PI as functions of temperature; (b) time- and temperature-dependent stress relaxation curves of DAS-Bio-PI; (c) weight loss curves of DAS-Bio-PI; (d) DTG curves of DAS-Bio-PI; (e and f) photographs of PP, PLA, and DAS-Bio-PI samples under 20 °C and 300 °C, respectively.

stability might be due to the incorporation of Priamine with inherent hydrophobicity into the DAS. DAS-Bio-PI films could also maintain the shapes and stiffness after soaking in most available organic solvents for 7 days (Fig. 5c), indicating the decent chemical resistances.

The chemical degradability of DAS-Bio-PI films was explored. Firstly, the acid degradation of DAS-Bio-PI film was proved to be feasible, albeit with limited efficiency. A complete degradation of DAS-Bio-PI film was observed after it was stirred repeatedly in a 5% acetic acid solution at room

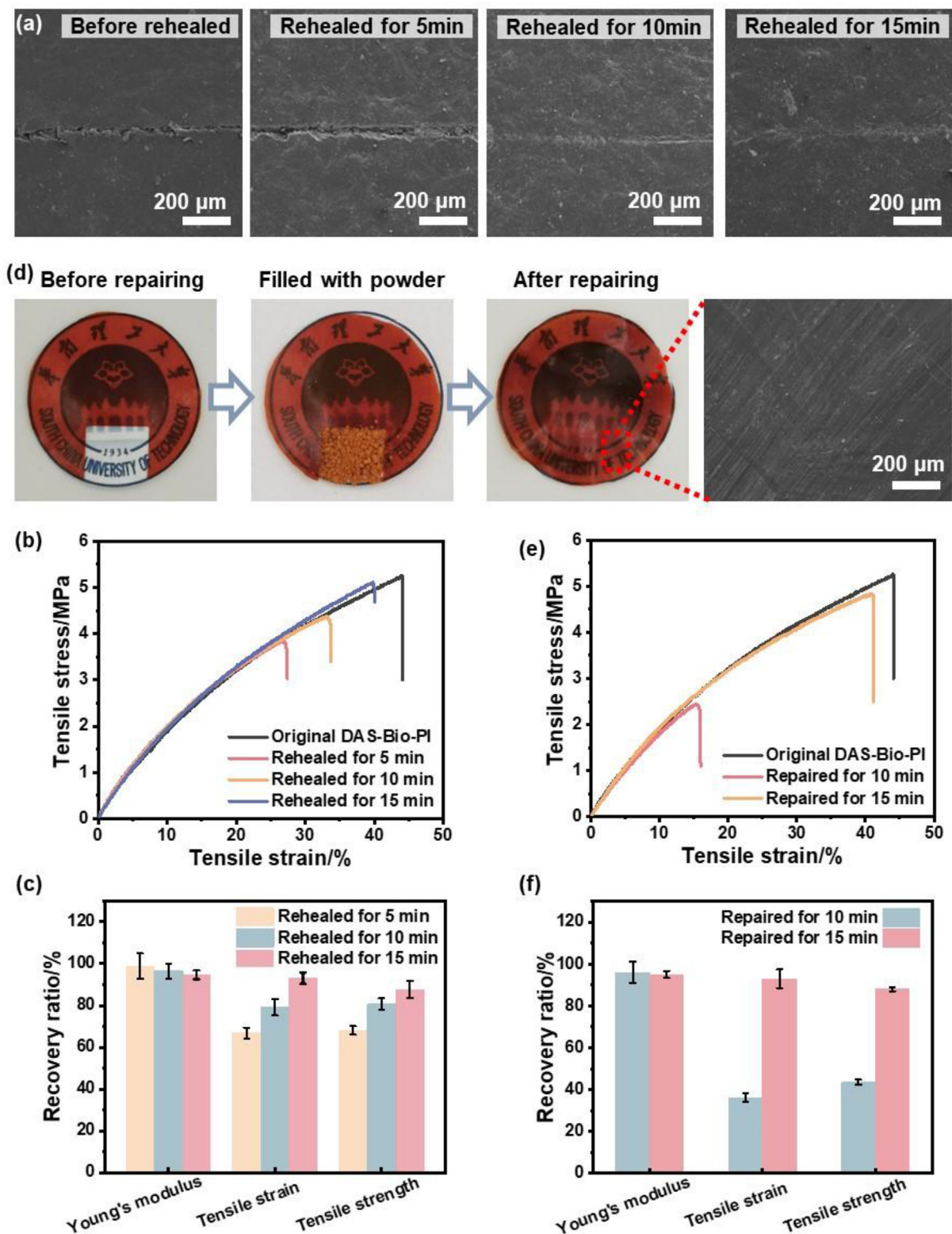


Fig. 4. Self-healing and large-area repairing ability of DAS-Bio-PI films. (a) SEM image of scratched DAS-Bio-PI film before reheating, reheated for 5 min, 10 min, and 15 min; (b) the tensile stress-strain curves and (c) recovery ratio of mechanical performance of reheated DAS-Bio-PI films; (d) the repaired process of DAS-Bio-PI film; (e) the tensile stress-strain curves and (f) recovery ratio of mechanical performance of repaired DAS-Bio-PI films.

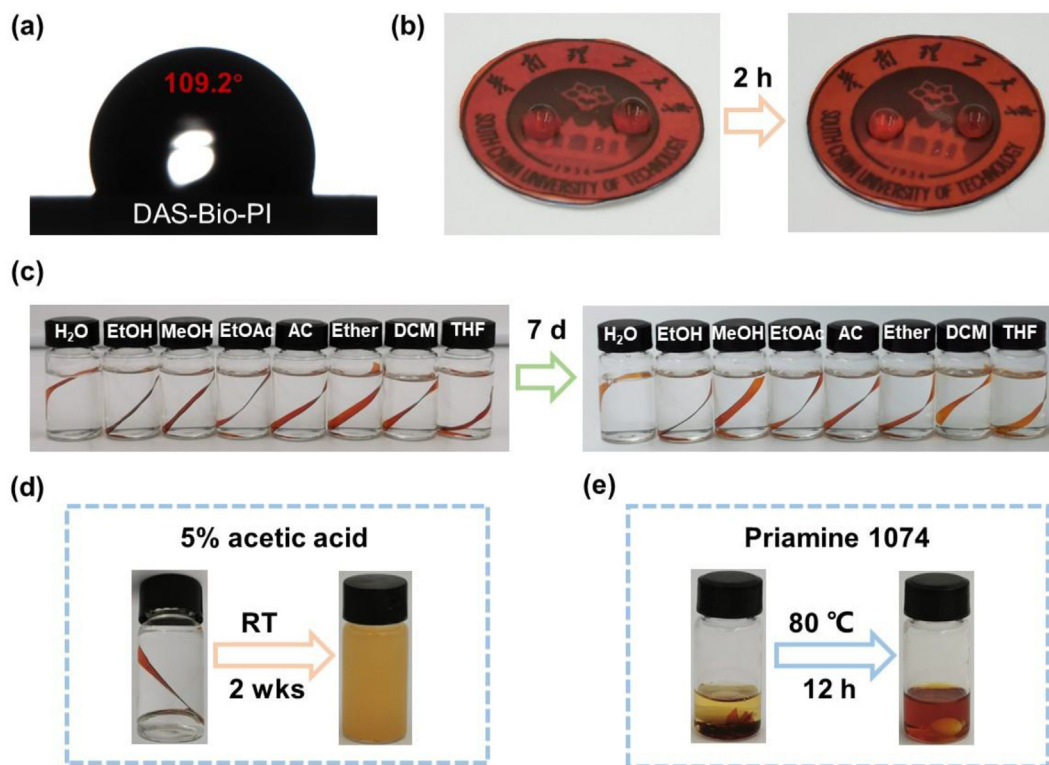


Fig. 5. Durability and degradability of DAS-Bio-PI. (a) The water contact angle and (b) waterproof performance of DAS-Bio-PI films; (c) the water and organic solvent resistance of DAS-Bio-PI films; the chemical degradation performance of DAS-Bio-PI films in (d) 5% acetic acid solution and in (e) Priamine 1074.

temperature for a duration of 2 weeks (Fig. 5d). Secondly, DAS-Bio-PI films were placed in Priamine 1074 at 80 °C. As investigated in previous reports, polyimine network could be chemically cleaved through disrupting balances between amino and aldehyde groups [38]. DAS-Bio-PI film was degraded after 12 h as anticipated (Fig. 5e), triggered by dynamic imine exchanges that breaking down the crosslinks.

3. Conclusions

In summary, we proposed a fully bio-based polyimine fabricated from natural starch and 100% renewable diamine monomer via dynamic imine chemistry. The stable dynamic imine crosslinking network endowed the obtained DAS-Bio-PI film with enhanced mechanical performances. The Young's modulus, elongation at break, and tensile strength of DAS-Bio-PI was 21.5 MPa, 45.2%, and 5.4 MPa, respectively. DAS-Bio-PI showed a good thermal processability because of the presence of large windows between T_g and decomposition temperature. Meanwhile, it exhibited superior stress relaxation properties and self-healing abilities due to the incorporation of dynamic imine network. A high flexibility, transparent, water and chemical resistance was also observed for DAS-Bio-PI. These properties make the fully bio-based DAS-Bio-PI described in this work attractive for practical applications such as petroleum-based plastics substitutes. Furthermore, this work presents a novel design strategy for CANs construction to develop sustainable, thermal processable, and degradable bioplastics fabricated from fully bio-based materials.

4. Experimental section

4.1. Materials

Dialdehyde starch (DAS, 90% starch oxidation, AR, Guangdong Wengjiang Chemical Reagent Co., Ltd), dimethyl sulfoxide (AR, Tianjin Fuyu Fine Chemicals Co., Ltd), ethanol (AR, Shanghai Titan Scientific Co., Ltd), and Priamine 1074 (CRODA, UK) were used as purchased.

4.2. Sample fabrication

A series of fully bio-based polyimines was fabricated by DAS and Priamine 1074 via Schiff base reactions. Different reacting ratios of aldehyde groups to amino groups were 1:1, 1:2, 1:3, and 1:4, which were expressed as DAS-Bio-PI-1, DAS-Bio-PI-2, DAS-Bio-PI-3, and DAS-Bio-PI-4, respectively. To describe the detailed hybridization procedure, DAS-Bio-PI-1 was used as an example. Firstly, 3 g of DAS was dissolved in 60 mL of DMSO. The solution was vigorously stirred at 100 °C for 2 h and then was cooled to 50 °C. After 9.95 g of Priamine 1074 was added, the mixture was reacted at 50 °C for 8 h with magnetic stirring to produce a reddish-brown gel. The gel was washed with ethanol and vacuum filtered to obtain reddish-brown solids. Finally, the solids were dried in a vacuum oven at 50 °C for 8 h after being volatilizing overnight. Dried DAS-Bio-PI-1 powders were grounded and then uniformly placed on mold (10 cm × 10 cm × 0.1 mm) with two pieces of PTFE film as substrate. It was heat-pressed

at 30 MPa for 15 min under 70 °C to get the DAS-Bio-PI-1 films by the flat-plate heat-pressing equipment.

4.3. Characterization methods

Fourier-transform infrared (FT-IR) analysis were obtained by a Tensor 27 FT-IR instrument within the range of 400–4000 cm^{-1} . X-ray diffraction (XRD) spectra were performed using a Smartlab 9 kW X-ray diffractometer (Rigaku, Japan). X-ray photoelectron spectroscopy (XPS) was conducted on an Axis Ultra DLD XPS instrument (Kratos, Britain). Morphological characteristics of samples were acquired using a Hitachi SU5000 (Japan) scanning electron microscope (SEM). The elemental mapping images of samples were investigated on an energy dispersive spectrometer (EDS) (GENESIS XM, Bruker, Germany). The mechanical properties and dynamic mechanical properties of DAS-Bio-PI films were tested using a mechanical testing instrument (Instron 5565, USA) and a dynamic mechanical analysis (DMA) instrument (TA Q800, USA), respectively. The thermal stability of DAS-Bio-PI films were analyzed using a NETZSCH TGA instrument (Germany) under nitrogen atmosphere.

Declaration of competing interest

The authors declare that they have no known competing financial interests or personal relationships that could have appeared to influence the work reported in this paper.

Acknowledgements

This work is supported by the National Natural Science Foundation of China (32171721, 22208131, 52103109), Guangdong Province Basic and Application Basic Research Fund (2023B1515040013), the State Key Laboratory of Pulp & Paper Engineering (2022C01, 202209).

Appendix A. Supplementary data

Supplementary data to this article can be found online at <https://doi.org/10.1016/j.gee.2023.08.002>.

References

- [1] Nat. Commun. 9 (2018) 2157.
- [2] A. Sangroniz, J.-B. Zhu, X. Tang, A. Etxeberria, E.Y.X. Chen, H. Sardon, Nat. Commun. 10 (2019) 3559.
- [3] J.R. Jambeck, R. Geyer, C. Wilcox, T.R. Siegler, M. Perryman, A. Andrady, R. Narayan, K.L. Law, Science 347 (2015) 768–771.
- [4] W. Leal Filho, U. Saari, M. Fedoruk, A. Iital, H. Moora, M. Klöga, V. Voronova, J. Clean. Prod. 214 (2019) 550–558.
- [5] M.K. Marichelvam, M. Jawaid, M. Asim, Fibers 7 (2019) 32.
- [6] J. Jeya Jeevahan, M. Chandrasekaran, S.P. Venkatesan, V. Sriram, G. Britto Joseph, G. Mageshwaran, R.B. Durairaj, Trends Food Sci. Technol. 100 (2020) 210–222.
- [7] H. Cheng, L. Chen, D.J. McClements, T. Yang, Z. Zhang, F. Ren, M. Miao, Y. Tian, Z. Jin, Trends Food Sci. Technol. 114 (2021) 70–82.
- [8] N.L. Tai, M. Ghasemlou, R. Adhikari, B. Adhikari, Carbohydr. Polym. 265 (2021) 118029.
- [9] M.I. Din, T. Ghaffar, J. Najeed, Z. Hussain, R. Khalid, H. Zahid, Food Addit. Contam. 37 (2020) 665–680.
- [10] E. Ojogbo, E.O. Ogunsona, T.H. Mekonnen, Materials Today Sustainability 7–8 (2020) 100028.
- [11] B. Biduski, F.T.D. Silva, W.M.D. Silva, S.L.D.M.E. Halal, V.Z. Pinto, A.R.G. Dias, E.D.R. Zavareze, Food Chem. 214 (2017) 53–60.
- [12] N. Masina, Y.E. Choonara, P. Kumar, L.C. Du Toit, M. Govender, S. Indermun, V. Pillay, Carbohydr. Polym. 157 (2017) 1226–1236.
- [13] P. Kanmani, J.-W. Rhim, Carbohydr. Polym. 106 (2014) 190–199.
- [14] M.I. Din, R. Sehar, Z. Hussain, R. Khalid, A.T. Shah, Inorg. Nano-Metal Chem. 51 (2021) 985–994.
- [15] X. Zhai, W. Wang, H. Zhang, Y. Dai, H. Dong, H. Hou, Carbohydr. Polym. 239 (2020) 116231.
- [16] C.C. Chang, B.M. Trinh, T.H. Mekonnen, J. Colloid Interface Sci. 593 (2021) 290–303.
- [17] F.M. Fakhouri, S. Maria Martelli, L. Canhadas Bertan, F. Yamashita, L.H. Innocentini Mei, F.P. Collares Queiroz, Lebensm. Wiss. Technol. 49 (2012) 149–154.
- [18] N. Nordin, S.H. Othman, S.A. Rashid, R.K. Basha, Food Hydrocolloids 106 (2020) 105884.
- [19] Y. Jin, Z. Lei, P. Taynton, S. Huang, W. Zhang, Matter 1 (2019) 1456–1493.
- [20] Z. Su, S. Huang, Y. Wang, H. Ling, X. Yang, Y. Jin, X. Wang, W. Zhang, J. Mater. Chem. A 8 (2020) 14082–14090.
- [21] Z. Lei, H. Chen, C. Luo, Y. Rong, Y. Hu, Y. Jin, R. Long, K. Yu, W. Zhang, Nat. Chem. 14 (2022) 1399–1404.
- [22] P. Taynton, K. Yu, R.K. Shoemaker, Y. Jin, H.J. Qi, W. Zhang, Adv. Mater. 26 (2014) 3938–3942.
- [23] Q. Zhao, M. Zhang, F. Song, Y. Xue, Z. Pan, Y. Zhou, Cell Rep. Phys. Sci. 4 (2023) 101244.
- [24] L.M. Sridhar, M.O. Oster, D.E. Herr, J.B.D. Gregg, J.A. Wilson, A.T. Slark, Green Chem. 22 (2020) 8669–8679.
- [25] B. Briou, B. Ameduri, B. Boutevin, Chem. Soc. Rev. 50 (2021) 11055–11097.
- [26] W.A. Ogden, Z. Guan, J. Am. Chem. Soc. 140 (2018) 6217–6220.
- [27] W.B. Ying, Z. Yu, D.H. Kim, K.J. Lee, H. Hu, Y. Liu, Z. Kong, K. Wang, J. Shang, R. Zhang, J. Zhu, R.-W. Li, ACS Appl. Mater. Interfaces 12 (2020) 11072–11083.
- [28] C. He, S. Shi, D. Wang, B.A. Helms, T.P. Russell, J. Am. Chem. Soc. 141 (2019) 13753–13757.
- [29] L. Lu, J. Fan, G. Li, Polymer 105 (2016) 10–18.
- [30] M.E. Belowich, J.F. Stoddart, Chem. Soc. Rev. 41 (2012) 2003–2024.
- [31] F. Song, Z. Li, P. Jia, M. Zhang, C. Bo, G. Feng, L. Hu, Y. Zhou, J. Mater. Chem. A 7 (2019) 13400–13410.
- [32] M.A. Rashid, S. Zhu, Q. Jiang, Y. Wei, W. Liu, ACS Appl. Polym. Mater. 5 (2023) 279–289.
- [33] H. Zhang, Z. Su, X. Wang, ACS Sustainable Chem. Eng. 10 (2022) 8650–8657.
- [34] J. Yu, P.R. Chang, X. Ma, Carbohydr. Polym. 79 (2010) 296–300.
- [35] J. Dahlke, S. Zechel, M.D. Hager, U.S. Schubert, Adv. Mater. Interfac. 5 (2018) 1800051.
- [36] J. Liu, K. Wang, Y. Xie, F. Gao, Q. Zeng, Y. Yuan, R. Liu, X. Liu, J. Coating Technol. Res. 14 (2017) 1325–1334.
- [37] C. Duval, N. Kébir, R. Jauseau, F. Burel, J. Polym. Sci., Part A: Polym. Chem. 54 (2016) 758–764.
- [38] P. Taynton, H. Ni, C. Zhu, K. Yu, S. Loob, Y. Jin, H.J. Qi, W. Zhang, Adv. Mater. 28 (2016) 2904–2909.
- [39] Q. Zhao, M. Zhang, S. Gao, Z. Pan, Y. Xue, P. Jia, C. Bo, Z. Luo, F. Song, Y. Zhou, J. Mater. Chem. A 10 (2022) 11363–11374.